Available online at www.ijournalse.org

Emerging Science Journal

(ISSN: 2610-9182)

Vol. 9, No. 1, February, 2025

Stochastic Diffusive Modeling of CO_2 Emissions with Population and Energy Dynamics

Muhammad Shoaib Arif [1, 2*], Kamaleldin Abodayeh [1], Hisham M. Al-Khawar [1], Yasir Nawaz [2]

[1] *Department of Mathematics and Sciences, College of Humanities and Sciences, Prince Sultan University, Riyadh, 11586, Saudi Arabia.*

[2] *Department of Mathematics, Air University, PAF Complex E-9, Islamabad, 44000, Pakistan.*

Abstract

Climate change, primarily driven by CO_2 emissions from energy and non-energy sectors, necessitates effective mitigation strategies. This study develops a stochastic diffusive model to capture the complex dynamics of CO_2 concentration, human population growth, and energy production. The objectives are to enhance the predictive accuracy of existing models by incorporating diffusion effects and stochastic variability, offering insights for sustainable environmental policies. A novel numerical scheme, an extension of the Euler-Maruyama algorithm, is proposed to solve stochastic time-dependent partial differential equations governing the model. The scheme's consistency and stability are rigorously analyzed in the mean square sense. Findings reveal that increasing emission rate coefficients in energy and non-energy sectors exacerbates CO_2 levels, emphasizing the need for stringent controls. The proposed scheme demonstrates superior accuracy to the non-standard finite difference method, establishing its efficacy in modeling complex environmental processes. This research contributes a robust computational tool to improve existing predictive models, aiding decision-making for long-term ecological sustainability. By addressing uncertainties in the environmental process, the work advances the understanding of interactions between population growth, energy production, and CO_2 emissions, offering a significant improvement over the traditional modeling approach. The novelty lies in integrating stochastic dynamics with diffusion to better inform CO_2 reduction strategies.

Keywords:

Stochastic Diffusive Model;
Consistency;
Stability; Existence;
CO_2 Emissions Reduction;
Diffusion Processes;
Environmental Uncertainty
Population Dynamics.

Article History:

Received:	13	September	2024
Revised:	10	December	2024
Accepted:	23	December	2024
Published:	01	February	2025

1- Introduction

Effective mitigation measures to address the growing levels of CO_2 in the atmosphere and their consequences on climate change have been an area of extensive research. We must have a deep understanding of the dynamic interplay of CO_2 emissions, the size of the population, and the energy we use to deal with this complex situation. The ways to establish the relationships between these three entities are dealt with in this paper. We first illustrate the nature of this relationship using a math model, which tries to conceptualize the system's fundamental complexity.

A suggested plan for using a differential equation model to analyze variations of CO_2 levels, population size, and energy usage over time. This model is developed based on the conventional differential equations controlling the shift of CO_2, population, and energy consumption. It also has some significant parameters in its equation, including growth rates, carrying capacity, mortality rates, and the efficacy of mitigation strategies over time. The need for energy is rising and will remain as long as the population keeps expanding. Carbon dioxide, a greenhouse gas, is added to the atmosphere due to the combustion of fossil fuels, which provide a large amount of the world's energy. Reduced carbon dioxide emissions from the energy sector are essential to achieving our goal of reducing the impact of climate change.

* **CONTACT**: marif@psu.edu.sa

DOI: http://dx.doi.org/10.28991/ESJ-2025-09-01-012

Mathematical models are increasingly used as potent tools to explain complex real-world processes (problems) clearly and concisely. Researchers have organized and thoroughly examined the relevant field in the last several decades. A mathematical equation can model a real-world process for future planning, prediction, etc. Mathematical tools can create various management strategies for studying, controlling, and eliminating infectious diseases. Over the past few decades, mathematical modeling and mathematical biology have been increasingly popular among scholars thanks to the many practical applications of these fields. Tian et al. [1] presented a mathematical model employing extended Monod growth kinetics and impulsive state feedback control, grounded in the design principles of a continuous bioprocess for regulating biomass concentration. The goal of establishing and investigating piecewise chemostat models with two thresholds is to keep the concentration of microorganisms within an acceptable range [2]. Both deterministic and stochastic models have been established to elucidate the macroscopic kinematics of chemical processes [3]. Zhao et al. [4] examined a chemostat model incorporating time delay and periodically pulsed input. When the impulsive effect duration is smaller than a critical value, we demonstrate that a periodic solution devoid of microorganisms is globally desirable.

Researchers have used ordinary calculus to represent real-world phenomena mathematically in a sequential fashion, and this is a crucial point to note. Fractional calculus drew academics because conventional models based on integrals or ordinary derivatives failed to describe practical issues adequately. Many of the features of mathematical models still defy satisfactory explanations by classical calculus. Thus, non-integer order derivatives can shed light on memory and inheritance in a more comprehensive way. In this case, previous studies were examined to provide an extensive introduction, background material, and critical conclusions regarding the utilization of these derivatives [5-8]. The complete range of a function is shown by its real or complex order derivatives. With one notable exception, the spectrum includes the corresponding integer counterpart. The number of degrees of freedom provided by fractional differential operators is more than that of integer orders. Furthermore, previous studies [9–12] are cited for the extensive usage of this field in addressing a wide range of practical issues.

Inspired by the uses mentioned above of operators, we look into the energy sectors' CO_2 emissions. The growth of a nation's energy sector is indicative of its overall socioeconomic status. As the world's population and economy expand, so does the energy industry. Between 2010 and 2040, global energy use is anticipated to increase by 56% [13]. According to reports, eighty percent of the world's energy comes from burning fossil fuels, such as coal, gas, oil, etc. [14]. In 2017, the United States was responsible for fifteen percent of the total greenhouse gas emissions produced worldwide, as stated in the U.S. Environmental Protection Agency [15]. The energy demand is directly proportional to the growth in the population. As a result, most nations meet their energy needs with nuclear power or fossil fuels, allowing their economies to grow steadily. However, fossil fuels are the main culprits since they release massive amounts of CO_2 into the atmosphere, increasing air pollution and decreasing oxygen levels. The rationale above is responsible for the recent climate change that has caused numerous destructions in the form of massive floods and earthquakes. Growing populations drive up primary energy demand, but affordable and reliable energy is critical to improving people's quality of life and driving economic expansion. Access to energy is a crucial factor in population growth. Improvements in energy quality and quantity made possible by technological advancements contributed to the Industrial Revolution, increasing productivity and the human population. Power consumption is another factor that affects population carrying capacity. Energy consumption and the population's carrying capacity are being raised by the development of new energy sources and technologies [16]. As a result of climate change, people are more likely to get sick from various sources, including contaminated food and water, extreme heat, and pollution. Reducing the harmful impacts of global warming requires significantly reducing CO_2 emissions from energy use [17]. Emami et al. [18] and Weng et al. [19] provide more relevant literature on transportation-related CO_2 emissions and their effects on energy resources.

Despite the availability of several mitigation strategies to reduce CO_2 emissions from the energy sector, the sector's continuous growth makes it challenging to achieve the mitigation targets. Reducing environmental CO_2 levels is becoming more difficult as the human population rises. Numerous statistical, semi-statistical, and empirical models are used to study energy management and CO_2 emission reduction on a national and regional scale. Qualitative analytical models can show how mitigation methods reduce energy sector carbon dioxide emissions. Previous studies [20-22] are used to cite studies investigating different mathematical models in this area.

The sustainable development of the urban power sector encounters tremendous obstacles due to the limitations imposed by traditional energy supplies and environmental space. When it comes to lowering the use of conventional energy resources and enhancing the mitigation of CO_2 emissions, renewable energy generation, and carbon capture and storage (CCS) are appealing technologies.

Several academics have proposed solutions to lower the power sector's CO_2 emissions. One example is the study of Beér [23], who stated that increasing plant efficiency, both new and old, is a crucial practical instrument for lowering CO_2 emissions from fossil fuel power stations shortly. Liu et al. [24] state that renewable energy sources have the potential to decrease carbon dioxide emissions significantly and are crucial in China's attempts to control greenhouse gas emissions from the power system. Carbon Capture and Storage (CCS) in the electricity industry was proposed by Jin et al. [25] and Yoro & Sekoai [26] as a viable technique for lowering greenhouse gas emissions in light of concerns about climate change. The ongoing process of the sociotechnical transition towards smart grids is contended by Mesarić et al. [27]. Smart grids can reduce energy consumption and mitigate carbon by avoiding electricity waste. This is made possible by improving performance reliability and customer responsiveness and encouraging more efficient decisions by both customers and the utility provider [28]. A novel energy system that incorporates thermal, gas, and electrical networks was suggested by Shi et al. [29] and is known as an energy systems integration (ESI) operational scheduling model.

Stochastic modeling is extensively employed in illness research because it yields more thorough insights than deterministic models. Unlike deterministic models, which can only use inputs to make predictions, stochastic models take outputs into account. To understand how epidemics spread, scientists have proposed using stochastic equations [30-33]. Scholars have also looked at the dynamic features of delays by including them in population interaction models [34-36].

There are two primary categories of mathematical models: deterministic and stochastic. Advances in both theory and computation have resulted from combining stochastic and deterministic models. Many people find deterministic models more straightforward to work with than stochastic ones.

Nevertheless, when assessing knockoffs, stochastic models offer a degree of impracticality. Unpredictable events often involve noise and random fluctuations, which is why stochastic models are used [37-42]. The fact that these models faithfully portray biological and natural events gives them a leg up over competing models [43-46]. Aspects of the engineering and natural science fields can be better understood with the help of stochastic models. They can be used to analyze rate changes, evaluate the effects of economic risks, and address difficulties [47, 48]. Furthermore, we can use them to study the unpredictable nature of healthcare systems. Deterministic methods, in contrast, are easier to grasp yet inaccurate.

***Identifying Gaps in the Literature*:** The majority of the research on CO_2 reduction strategies is based on deterministic models that ignore the fact that environmental systems are inherently uncertain. Although there are stochastic models, they usually only include certain parts of the equation, such as CO_2 emissions or population dynamics, not how these elements interact with energy production. Also, in real-world situations, the geographic dispersion of CO_2 across regions is greatly influenced by the effects of diffusion, which are mostly ignored in most research. Stochastic differential equations, including randomness and diffusion, are difficult to solve using traditional numerical methods like the Euler-Maruyama algorithm. Also, many models ignore these variables' unpredictable and dynamic character in connection to energy dynamics and population expansion by treating energy and non-energy sector emissions independently or assuming constant emission rates. Current models for long-term CO_2 reduction plans are not as accurate or applicable due to these constraints.

Proposing Our Approach to Fill These Gaps: To fill these gaps, our research suggests a full stochastic diffusive model that takes into consideration CO_2 concentration, population dynamics, energy generation, spatial diffusion, and stochastic uncertainty. Our model better captures the dynamic interplay between the energy and non-energy sectors' emission rates by including random fluctuations in both rates. Moreover, the model incorporates diffusion, an important but sometimes ignored phenomenon in earlier research, enabling more precise predictions of CO_2 dispersion. To guarantee precise predictions, we enhance the stability and accuracy of the Euler-Maruyama approach for complicated stochastic differential equations. Thanks to this adjustment, we are better equipped to deal with the difficulties caused by diffusion and unpredictability. Furthermore, our model is the first to integrate stochastic dynamics, diffusion, and emissions from the energy sector into a unified framework. This makes it a more accurate and trustworthy tool for predicting CO_2 levels and directing successful reduction strategies, which in turn helps ensure ecological sustainability in the long run.

Our work primarily revolves around advancing a sophisticated numerical technique that may be seen as an expansion of the widely recognized Euler-Maruyama approach. Stochastic time-dependent partial differential equations are commonly used in environmental modeling to portray complex systems' uncertainties and random fluctuations accurately. The suggested approach can effectively handle stochastic equations and demonstrates consistency and stability in the mean square sense. This makes it a trustworthy and accurate foundation for simulations.

We modified a previous mathematical model that included diffusion and random fluctuations to better represent the relationship between CO_2 concentration, population dynamics, and energy production. Incorporating stochastic components and diffusion effects into simulations of environmental processes helps us comprehend their dynamic interactions, allowing us to simulate real-world events more accurately.

We may test our computing method by solving the updated mathematical model and comparing the results to a non-standard finite difference method. The assessment examines numerical precision and energy and non-energy sector emission rate coefficients on carbon dioxide concentration. According to our results, the stochastic scheme is more accurate and reliable than the non-standard finite difference method.

2- Proposed Computational Scheme

The numerical technique consists of two stages: the predictor stage, also known as the first stage, identifies the solution at any time level, while the second stage identifies the solution at the $(n+1)th$ time level, taking into account the known solution at the nth level. To propose a scheme, consider the Equation.

$$\frac{\partial f}{\partial t} = d_1 \frac{\partial^2 f}{\partial x^2} + G(f) \tag{1}$$

The initial phase of the scheme for Equation 1 is expressed as:

$$\bar{f}_i^{n+1} = f_i^n + c\Delta t \left.\frac{\partial f}{\partial t}\right|_i^n \tag{2}$$

where Δt is a time step size.

Now, the second phase of the scheme is indicated by the following:

$$f_i^{n+1} = \frac{1}{3}\left(2f_i^n + \bar{f}_i^{n+1}\right) + a\Delta t \left.\frac{\partial f}{\partial t}\right|_i^n + b\Delta t \left.\frac{\partial \bar{f}}{\partial t}\right|_i^{n+1} \tag{3}$$

Now, substituting Equation 2 into Equation 3 it is obtained:

$$f_i^{n+1} = \frac{1}{3}\left(3f_i^n + c\Delta t \left.\frac{\partial f}{\partial t}\right|_i^n\right) + a\Delta t \left.\frac{\partial f}{\partial t}\right|_i^n + b\Delta t \left.\frac{\partial f}{\partial t}\right|_i^n + bc(\Delta t)^2 \left.\frac{\partial^2 f}{\partial t^2}\right|_i^n \tag{4}$$

Re-write Equation 4 as:

$$f_i^{n+1} = f_i^n + \frac{c}{3}\Delta t \left.\frac{\partial f}{\partial t}\right|_i^n + (b+a)\Delta t \left.\frac{\partial f}{\partial t}\right|_i^n + bc(\Delta t)^2 \left.\frac{\partial^2 f}{\partial t^2}\right|_i^n \tag{5}$$

The Taylor series expansion for f_i^{n+1} is given as:

$$f_i^{n+1} \approx f_i^n + \Delta t \left.\frac{\partial f}{\partial t}\right|_i^n + \frac{(\Delta t)^2}{2} \left.\frac{\partial^2 f}{\partial t^2}\right|_i^n + O((\Delta t)^3) \tag{6}$$

By using a Taylor series expansion 6 into Equation 5 it yields:

$$f_i^n + \Delta t \left.\frac{\partial f}{\partial t}\right|_i^n + \frac{(\Delta t)^2}{2} \left.\frac{\partial^2 f}{\partial t^2}\right|_i^n = f_i^n + \left(a + b + \frac{c}{3}\right)\Delta t \left.\frac{\partial f}{\partial t}\right|_i^n + bc(\Delta t)^2 \left.\frac{\partial^2 f}{\partial t^2}\right|_i^n \tag{7}$$

By comparing coefficients of $\Delta t \left.\frac{\partial f}{\partial t}\right|_i^n$ and $(\Delta t)^2 \left.\frac{\partial^2 f}{\partial t^2}\right|_i^n$ on both sides of Equation 7 it yields:

$$\left.\begin{aligned} 1 &= a + b + \frac{c}{3} \\ \frac{1}{2} &= bc \end{aligned}\right\} \tag{8}$$

By solving a linear Equation 8 b and c can be found as:

$$b = \frac{1}{2c}, a = 1 - \frac{c}{3} - \frac{1}{2c} \tag{9}$$

So, the values of a and b depend on the value of c. There are several options to choose the value of c. Therefore, the time discretization of Equation 1 is:

$$\bar{f}_i^{n+1} = f_i^n + c\Delta t \left(d_1 \left.\frac{\partial^2 f}{\partial t^2}\right|_i^n + G(f_i^n)\right) \tag{10}$$

$$f_i^{n+1} = \frac{1}{3}\left(2f_i^n + \bar{f}_i^{n+1}\right) + \Delta t \left\{a\left(d_1 \left.\frac{\partial^2 f}{\partial t^2}\right|_i^n + G(f_i^n)\right) + b\left(d_1 \left.\frac{\partial^2 \bar{f}}{\partial t^2}\right|_i^{n+1} + G\left(\bar{f}_i^{n+1}\right)\right)\right\} \tag{11}$$

Let the second-order central difference formula for the spatial term the fully discretized scheme be written as:

$$\bar{f}_i^{n+1} = f_i^n + c\Delta t\left(d_1 \delta_x^2 f_i^n + G(f_i^n)\right) \tag{12}$$

$$f_i^{n+1} = \frac{1}{3}\left(2f_i^n + \bar{f}_i^{n+1}\right) + \Delta t \left\{a\left(d_1 \delta_x^2 f_i^n + G(f_i^n)\right) + b\left(d_1 \delta_x^2 \bar{f}_i^{n+1} + G\left(\bar{f}_i^{n+1}\right)\right)\right\} \tag{13}$$

Now consider the partial differential Equation as:

$$df = d_1 \partial_{xx} f dt + G(f)dt + \sigma f dW \tag{14}$$

where $W(t)$ is a Wiener process.

The difference Equation when the proposed scheme discretizes Equation 14 is given as:

$$f_i^{n+1} = \frac{1}{3}\left(2f_i^n + \bar{f}_i^{n+1}\right) + \Delta t\left\{a\left(d_1\delta_x^2 f_i^n + G(f_i^n)\right) + b\left(d_1\delta_x^2\bar{f}_i^{n+1} + G\left(\bar{f}_i^{n+1}\right)\right)\right\} + \sigma f_i^n\Delta W \tag{15}$$

where $\Delta W \sim W^{n+1} - W^n$ is approximated by Normal distribution $N(0,\Delta t)$, and the first stage is the same as for the deterministic model.

Theorem 1: The proposed computational scheme 12 and 15 is consistent in the mean square sense for Equation 14 with $G = 0$.

Proof: Let F be the smooth function and $L(F)_i^n, L_i^n(F)$ are continuous and discrete operators, then:

$$L(F)_i^n = F\big((n+1)\Delta t, i\Delta x\big) - F(n\Delta t, i\Delta x) - d_1\int_{n\Delta t}^{(n+1)\Delta t} F_{xx}(s, i\Delta x)ds - \sigma\int_{n\Delta t}^{(n+1)\Delta t} F(s, i\Delta x)dW(s) \tag{16}$$

$$L_i^n F = F\big((n+1)\Delta t, i\Delta x\big) - F(n\Delta t, i\Delta x) - \frac{\Delta t}{(\Delta x)^2}\Big[d_1\left(a + b + \frac{c}{3}\right)\big(F(n\Delta t,(i+1)\Delta x) - 2F(n\Delta t, i\Delta x) + F(n\Delta t,(i-1)\Delta x)\big) + bc\big(F(n\Delta t,(i+2)\Delta x) - 4F(n\Delta t,(i+1)\Delta x) + 6F(n\Delta t, i\Delta x)\big) - 4F(n\Delta t,(i-1)\Delta x) + F(n\Delta t,(i-2)\Delta x)\Big] - \sigma F(n\Delta t, i\Delta x)\Big(W\big((n+1)\Delta t\big) - W(n\Delta t)\Big) \tag{17}$$

It is obtained by subtracting Equation 17 from Equation 16 and applying the square of expected value for the absolute value of difference.

$$E|L(F)_i^n - L_i^n F|^2 = E\,\Big|-d_1\int_{n\Delta t}^{(n+1)\Delta t} F_{xx}(s, i\Delta x)ds + \frac{\Delta t}{(\Delta x)^2}\Big(\left(a + b + \frac{c}{3}\right)d_1 F(n\Delta t,(i+1)\Delta x) - 2F(n\Delta t, i\Delta x) + F(n\Delta t, i\Delta x) + bc\big(F(n\Delta t,(i+2)\Delta x) - 4F(n\Delta t,(i+1)\Delta x) + 6F(n\Delta t, i\Delta x)\big) - 4F(n\Delta t,(i-1)\Delta x) + F(n\Delta t,(i-2)\Delta x)\Big) - \sigma\int_{n\Delta t}^{(n+1)\Delta t} F(s, i\Delta x)dW(s) + \sigma F(n\Delta t, i\Delta x)\Big(W\big((n+1)\Delta t\big) - W(n\Delta t)\Big)\Big|^2 \tag{18}$$

Equation 18 can be reduced to the following inequality:

$$E|L(F)_i^n - L_i^n F|^2 \le 2d_1^2 E\,\Big|\int_{n\Delta t}^{(n+1)\Delta t} F_{xx}(s, i\Delta x)ds - \frac{\Delta t}{(\Delta x)^2}\Big\{\left(a + b + \frac{c}{3}\right)\big(F(n\Delta t,(i+1)\Delta x) - 2F(n\Delta t, i\Delta x) + F(n\Delta t,(i-1)\Delta x)\big) - bc\big(F(n\Delta t,(i+2)\Delta x) - 4F(n\Delta t,(i+1)\Delta x) + 6F(n\Delta t, i\Delta x)\big) - 4F(n\Delta t,(i-1)\Delta x) + F(n\Delta t,(i-2)\Delta x)\Big\}\Big|^2 + 2\sigma^2 E\,\Big|\int_{n\Delta t}^{(n+1)\Delta t} F(s, i\Delta x)dW(s) + F(n\Delta t, i\Delta x)dW(S)\Big|^2 \tag{19}$$

By using the following inequality:

$$E\left|\int_{t_\circ}^{t} g(s,j)dW(S)\right|^{2m} \le (t - t_\circ)^{m-1}[m(2m-1)]^m\int_{t_\circ}^{t} E[|g(s,j)|^{2m}]ds \tag{20}$$

The following inequality can be obtained using inequality 20 into 19.

$$E|L(F)_i^n - L_i^n F|^2 \le 2d_1^2 E\,\Big|\int_{n\Delta t}^{(n+1)\Delta t} F_{xx}(s, i\Delta x)ds - \frac{\Delta t}{(\Delta x)^2}\Big\{\left(a + b + \frac{c}{3}\right)\big(F(n\Delta t,(i+1)\Delta x) - 2F(n\Delta t, i\Delta x) + F(n\Delta t,(i-1)\Delta x)\big) - bc\big(F(n\Delta t,(i+2)\Delta x) - 4F(n\Delta t,(i+1)\Delta x) + 6F(n\Delta t, i\Delta x)\big) - 4F(n\Delta t,(i-1)\Delta x) + F(n\Delta t,(i-2)\Delta x)\Big\}\Big|^2 + 2\sigma^2\int_{n\Delta t}^{(n+1)\Delta t} E|-F(s, i\Delta x) + F(n\Delta t, i\Delta x)|^2 ds \tag{21}$$

Thus, applying the limit when $\Delta x \to 0, \Delta t \to 0$ and $(n\Delta t, i\Delta x) \to (t, x)$ then:

$$E|L(F)_i^n - L_i^n F|^2 \to 0$$

Hence, the proposed stochastic computational scheme is consistent in the mean square sense.

Theorem 2: The proposed stochastic computational scheme is conditionally stable in mean square sense for Equation 14 for $G = 0$.

Proof: The stability condition of the proposed strategy will utilize Fourier series analysis. To do that, consider the following transformations:

$$\left.\begin{aligned} \bar{f}_i^{n+1} = \bar{P}^{n+1}e^{iI\psi}, f_i^{n+1} = P^{n+1}e^{iI\psi} \\ f_{i\pm1}^n = P^n e^{(i\pm1)I\psi}, f_i^n = P^{n+1}e^{iI\psi} \end{aligned}\right\} \tag{22}$$

where $I = \sqrt{-1}$.

By using the corresponding transformations from Equation 22 into the first stage of the proposed scheme 12 with $G = 0$, it yields.

$$\bar{P}^{n+1}e^{iI\psi} = P^n e^{iI\psi} + \frac{d_1\Delta t}{(\Delta x)^2}\left(e^{(i+1)I\psi} - 2e^{iI\psi} + e^{(i-1)I\psi}\right)P^n \tag{23}$$

Dividing both sides of Equation 23 by $e^{iI\psi}$ that yields:

$$\bar{P}^{n+1} = P^n + c\frac{d_1\Delta t}{(\Delta x)^2}\left(e^{I\psi} - 2 + e^{-I\psi}\right)P^n \tag{24}$$

Using De Movier's Theorem, Equation 24 can be expressed as:

$$\bar{P}^{n+1} = P^n + 2dd_1c(cos\psi - 1) \tag{25}$$

where $d = \frac{\Delta t}{(\Delta x)^2}$.

Similarly, by using relevant transformations from Equation 22 into Equation 15 with $G = 0$ it yields.

$$P^{n+1} = \frac{1}{3}(2P^n + \bar{P}^{n+1}) + d\{2a(cos\psi - 1)P^n + 2bd(cos\psi - 1)\bar{P}^{n+1}\} + \sigma P^n \Delta W \tag{26}$$

Upon substituting Equation 25 into Equation 26 that gives:

$$P^{n+1} = \left[\frac{2}{3} + 2ad(cos\psi - 1)\right]P^n + (\frac{1}{3} + 2bd(cos\psi - 1)\left(1 + 2cd_1d(cos\psi - 1)\right)P^n \tag{27}$$

The amplification factor is given as:

$$\frac{P^{n+1}}{P^n} = \bar{a} \tag{28}$$

where $\bar{a} = \frac{2}{3} + 2ad(cos\psi - 1)$+ $(\frac{1}{3} + 2bd(cos\psi - 1)\left(1 + 2cd_1d(cos\psi - 1)\right)$.

In the mean square sense, Equation 28 can be written as:

$$E\left|\frac{P^{n+1}}{P^n}\right|^2 \leq E|\bar{a}|^2 + E|\sigma\Delta W|^2 \tag{29}$$

Let $|\sigma|^2 = \lambda$ and assume that $|\bar{a}| \leq 1$ the inequality 29 is expressed as:

$$E\left|\frac{P^{n+1}}{P^n}\right|^2 \leq 1 + \lambda\Delta t \tag{30}$$

Therefore, the proposed stochastic computational scheme is conditional stable in the mean square sense.

3- Mathematical Model

The proposed scheme will be applied to solve a diffusive carbon dioxide model. Its ordinary differential equation model was studied in Verma et al. [49]. The ordinary differential equation model is given as:

$$\frac{dC}{dt} = -\alpha(C - C_\circ) + \lambda_1 N + \lambda_2(1 - \mu_2)E \tag{31}$$

$$\frac{dN}{dt} = rN\left(1 - \frac{N}{L}\right) + \beta_1 NE + \beta_2 N^2 E - \theta(C - C_\circ)N \tag{32}$$

$$\frac{dE}{dt} = (1 - \mu_1)\frac{\gamma NE}{K+N} - \gamma_\circ E^2 \tag{33}$$

where $C(0) \geq C_\circ, N(0) \geq 0, E(0) \geq 0$ and C is used for the concentration of carbon dioxide $C_\circ$ is pre-industrial CO_2 concentration, λ_1 is used for emission rate coefficients of CO_2 in the non-energy sector, λ_2 represents emission rate coefficients of CO_2 in the energy sector, the parameter μ_2 represents the efficiency of mitigation options to curtail the CO_2 emission rate per unit of energy use, N is used to represent the human population, r is the intrinsic growth rate, L is the carrying capacity of the population, α represents the removal rate of atmospheric CO_2 by the sinks of CO_2, carrying capacity of the population due to energy use, θ is used for mortality rate coefficients of the population due to adverse impact imposed by enhanced CO_2 level, E represents the energy used, γ represents the growth rate of energy use, K is used for the half-saturation constant, which represents the population at which the growth rate of energy use is half of its maximum level, $\gamma_\circ$ represents the depletion rate of energy use, μ_1 represents the efficiency of mitigation options to reduce energy consumption by increasing energy efficiency and bringing behavioural changes in people.

The equilibrium points can be obtained as:

$$0 = -\alpha(C - C_\circ) + \lambda_1 N + \lambda_2(1 - \mu_2)E \tag{34}$$

$$0 = rN\left(1 - \frac{N}{L}\right) + \beta_1 NE + \beta_2 N^2 E - \theta(C - C_\circ)N \tag{35}$$

$$0 = (1 - \mu_1)\frac{\gamma NE}{K+N} - \gamma_\circ E^2 \tag{36}$$

One of the equilibrium points is written as:

$$C^* = \frac{\alpha C_\circ \gamma + L\lambda_1\gamma + C_\circ L\lambda_1\theta}{\alpha\gamma + L\lambda_1\theta}$$

$$N^* = \frac{\alpha L\gamma}{\alpha\gamma + L\lambda_1\theta}$$

$$E^* = 0$$

The system will remain stable if the eigenvalues of the following Jacobian matrix evaluated at the equilibrium point are negative.

$$\begin{bmatrix} -\alpha & \lambda_1 & \lambda_2(1-\mu_2) \\ \frac{-\alpha L\gamma\theta}{\alpha\gamma+L\lambda_1\theta} & \frac{-\alpha\gamma^2}{\alpha\gamma+L\lambda_1\theta} + \gamma\left(1 - \frac{\alpha\gamma}{\alpha\gamma+L\lambda_1\theta}\right) - \theta\left(-C_\circ + \frac{\alpha C_\circ\gamma + L\lambda_1 + C_\circ L\lambda_1\theta}{\alpha\gamma+L\lambda_1\theta}\right) & \frac{\alpha^2\beta_2 L^2\gamma^2}{(\alpha\gamma+L\lambda_1\theta)^2} + \frac{\alpha\beta l\gamma}{\alpha\gamma+L\lambda_1\theta} \\ 0 & 0 & \frac{\alpha\gamma L(1-\mu_1)}{(\alpha\gamma+L\lambda_1\theta)\left(K+\frac{\alpha L\gamma}{\alpha\gamma+L\lambda_1\theta}\right)} \end{bmatrix}$$

The diffusive stochastic model is proposed as:

$$dC = d_1\partial_{xx}C + (-\alpha(C - C_\circ) + \lambda_1 N + \lambda_2(1 - \mu_2)E) + \sigma_1 CW(t) \tag{37}$$

$$dN = d_2\partial_{xx}N + \left(rN\left(1 - \frac{N}{L}\right) + \beta_1 NE + \beta_2 N^2 E - \theta(C - C_\circ)N\right)dt + \sigma_2 NW(t) \tag{38}$$

$$dE = d_3\partial_{xx}E + \left((1 - \mu_1)\frac{\gamma NE}{K+N} - \gamma_\circ E^2\right)dt + \sigma_3 EW(t) \tag{39}$$

Subject to the boundary conditions:

$$\frac{\partial C}{\partial x} = 0,\ \frac{\partial N}{\partial x} = 0,\ \frac{\partial E}{\partial x} = 0 \tag{40}$$

The proposed diffusive stochastic model is a system of coupled partial differential equations (PDEs) that describes the dynamics of carbon dioxide concentration C, human population N, and energy production E while incorporating diffusion effects, deterministic dynamics, and stochastic variations. Below is a detailed explanation of each equation and the associated boundary conditions:

Carbon Dioxide Dynamics C Equation 37: Diffusion term $d_1\partial_{xx}C$: Models the spatial dispersion of CO_2, accounting for its spread over the region. Here d_1 is the diffusion coefficient. $-\alpha(C - C_\circ)$: represents the natural decay or absorption of CO_2 to a pre-industrial carbon dioxide concentration $C_\circ$. $\lambda_1 N$: models the concentration of the population N to CO_2emissions. $\lambda_2(1 - \mu_2)E$ represents the energy production E to CO_2 emission modulated by the efficiency factor $(1 - \mu_2)$. Stochastic term $\sigma_1 CW(t)$: introduce randomness in the emission process modelled using a Wiener process $W(t)$ with intensity σ_1 reflecting environmental uncertainties.

Population Dynamics Equation 38: Diffusion term $d_2\partial_{xx}N$: models spatial mitigation or the spread of the population. $\gamma N\left(1 - \frac{N}{L}\right)$ represents the logistic growth of the population with γ as a growth rate and L as a carrying capacity. $\beta_1 NE + \beta_2 N^2 E$: terms representing the impact of energy availability on population growth where β_1 and β_2 are interaction coefficients. $-\theta(C - C_\circ)N$: reflects the adverse effects of CO_2 concentration on population growth where θ quantifies this impact. Stochastic term $\sigma_2 NW(t)$: accounts for random fluctuation in population dynamics due to unpredictable factors with intensity σ_2.

Energy Production Dynamics Equation 39: Diffusion term $d_3\partial_{xx}E$: models the spatial diffusion of energy production activities. $(1 - \mu_1)\frac{\gamma NE}{K+N}$: represents energy production influenced by the population with $(1 - \mu_1)$ accounting for energy efficiency and K as population half-saturation coefficients. $\sigma_3 EW(t)$ capture random variations in energy production processes with intensity σ_3.

Boundary Conditions Equation 40: These Neumann boundary conditions specify that the flux of CO_2, population, and energy production at the boundaries of the spatial domain is zero. Physically, this means there is no inflow or outflow at the domain edges, ensuring that the system's dynamics are self-contained within the specified region.

This comprehensive model facilitates a detailed comprehension of the interrelated dynamics of CO_2, population, and energy E within realistic environmental contexts, providing it a useful tool for analyzing and formulating reduction strategies.

Theorem 3: Consider a convex, bounded, and closed set B in a Banach space $L_2((0,t) \times \Omega)$ and let V be a continuous function such that $f: B \to B$. Then f would have at least one fixed point if the image of the ball is pre-compact.

To prove the existence of the solution, consider the first linear stochastic partial differential Equation 37.

If f is twice the differential with respect to L_2- norm, Equation 37 can be expressed as a Volterra integral Equation.

$$f = f_\circ + \int_0^t d_1 \partial_{xx} C + (-\alpha(C - C_\circ) + \lambda_1 N + \lambda_2(1 - \mu_2)E)d\tau + \sigma_1 C W(t) \tag{41}$$

Re-write Equation 41 in operator form as:

$$T = f_\circ(x) + \int_0^t d_1 \partial_{xx} C + (-\alpha(C - C_\circ) + \lambda_1 N + \lambda_2(1 - \mu_2)E)d\tau + \sigma_1 C W(t) \tag{42}$$

To establish the existence of fixed-point operator f the mentioned Theorem 3 will be applied. According to the Theorem, each subset is closed, bounded, and convex in the function space. For small random variation dW a fixed-point operator will be integrated. The space $L_2[0,\zeta], \zeta = |t - 0|$ will be adopted for best perturbation.

Now a ball $\mathrm{B_r}(f_\circ)$ is constructed which is closed, bounded, and convex, which is center at the given initial condition as L_2function.

$$\mathrm{B_r}(f_\circ) = \{f \epsilon L_2[0,\zeta], \|f - f_\circ\|_{L_2[0,\zeta]} \leq \bar{r}\} \tag{43}$$

That gives $\|f\|_{L_2[0,\zeta]} \leq \bar{r} + f_\circ$ (44)

Within infinite-dimensional space, the convex, closed and bounded subsets exist, rendering it non-compact. Theorem 3 will be implemented if the following conditions are satisfied.

(i) $T: \mathrm{B_r}(f_\circ) \to \mathrm{B_r}(f_\circ)$.

(ii) $T(\mathrm{B_r}(f_\circ))$ is *pre*-compact.

Now $\|T - f_\circ\|_{L_2[0,\zeta]} = \left\| \int_0^t d_1 \partial_{xx} C + (-\alpha(C - C_\circ) + \lambda_1 N + \lambda_2(1 - \mu_2)E)d\tau + \sigma_1 C W(t) \right\|_{L_2[0,\zeta]}$ (45)

$$\|T - f_\circ\|_{L_2[0,\zeta]} \leq \int_0^t \left[d_1 \|\partial_{xx} C\|_{L_2[0,\zeta]} + \alpha \|C\|_{L_2[0,\zeta]} + \alpha C_\circ + \lambda_1 \|N\|_{L_2[0,\zeta]} + \lambda_2(1 - \mu_2)\|E\|_{L_2[0,\zeta]}\right] d\tau + |\sigma_1| \|C\|_{L_2[0,\zeta]} \int_0^t dW \tag{46}$$

$$\|T - f_\circ\|_{L_2[0,\zeta]} \leq \int_0^t \left[d_1 \bar{k} + \alpha(\bar{r} + c_1) + \alpha c_\circ + \lambda_1(\bar{r} + c_2) + \lambda_2 |1 - \mu| (\bar{r} + c_3)\right] d\tau + |\sigma_1| (\bar{r} + c_1) \int_0^t dW \tag{47}$$

$$\|T - f_\circ\|_{L_2[0,\zeta]} \leq \int_0^t \left[d_1 \bar{k} + \alpha(\bar{r} + c_1) + \alpha c_\circ + \lambda_1(\bar{r} + c_2) + \lambda_2 |1 - \mu| (\bar{r} + c_3)\right] d\tau + |\sigma_1| (\bar{r} + c_1)\big(W(t) - W(0)\big) \tag{48}$$

Since, $W(t)$ is a finite number, so:

$$\|T - f_\circ\|_{L_2[0,\zeta]} \leq \left[d_1 \bar{k} + \alpha(\bar{r} + c_1) + \alpha c_\circ + \lambda_1(\bar{r} + c_2) + \lambda_2 |1 - \mu| (\bar{r} + c_3)\right] \zeta + |\sigma_1| (\bar{r} + c_1) \beta_1 \zeta \tag{49}$$

For self-mapping:

$$\left[d_1 \bar{k} + \alpha(\bar{r} + c_1) + \alpha c_\circ + \lambda_1(\bar{r} + c_2) + \lambda_2 |1 - \mu| (\bar{r} + c_3)\right] \zeta + |\sigma_1| (\bar{r} + c_1) \beta_1 \zeta \ \leq \bar{r}$$

This implies $\zeta \leq \frac{\bar{r}}{[d_1 \bar{k} + \alpha(\bar{r} + c_1) + \alpha c_\circ + \lambda_1(\bar{r} + c_2) + \lambda_2 |1 - \mu| (\bar{r} + c_3)] + |\sigma_1| (\bar{r} + c_1) \beta_1}$.

The following approach will be useful for establishing the pre-compactness of T:

$$\|T_i(t) - T_i(t_1)\|_{L_2[0,\zeta]} \leq \int_t^{t_1} \big(d_1 \|\partial_{xx} C\|_{L_2[0,\zeta]} + \alpha \|C\|_{L_2[0,\zeta]} + \alpha C_\circ + \lambda_1 \|N\|_{L_2[0,\zeta]} + \lambda_2 |1 - \mu| \|E\|_{L_2[0,\zeta]} f\big) \zeta + |\sigma_1| \, \|C\|_{L_2[0,\zeta]} \int_t^{t_1} dW$$

$$\|T_i(t) - T_i(t_1)\|_{L_2[0,\zeta]} \leq \big(d_1 \|\partial_{xx} C\|_{L_2[0,\zeta]} + \alpha \|C\|_{L_2[0,\zeta]} + \alpha C_\circ + \lambda_1 \|N\|_{L_2[0,\zeta]} + \lambda_2 |1 - \mu| \|E\|_{L_2[0,\zeta]} f\big) \zeta (t_1 - t) + |\sigma_1| \|C\|_{L_2[0,\zeta]} (W(t_1) - W(t))$$

$$\|T_i(t) - T_i(t_1)\|_{L_2[0,\zeta]} \leq \big(d_1 \|\partial_{xx} C\|_{L_2[0,\zeta]} + \alpha \|C\|_{L_2[0,\zeta]} + \alpha C_\circ + \lambda_1 \|N\|_{L_2[0,\zeta]} + \lambda_2 |1 - \mu| \|E\|_{L_2[0,\zeta]} f\big) \zeta (t_1 - t) + |\sigma_1| \|C\|_{L_2[0,\zeta]} (t_1 - t)$$

Now, when $t \to t_1$ then $T_i(t) \to T_i(t_1)$. Therefore, it is proven that T_i has a uniformly convergent subsequence T_{i_n} of T_i. So $T\big(\mathrm{B_r}(f_\circ)\big)$ is pre-compact. Thus, according to Theorem 3, a fixed point function must exist. $\tilde{T}_i$of T_i which is also the solution of Equation 37.

4- Results and Discussion

Stochastic partial differential equations can be solved using the proposed scheme. It is suggested that the method be used with two separate PDEs. The first part of the scheme is constructed for a deterministic partial differential equation, and the second part deals with the stochastic part of the stochastic partial differential equation. The whole scheme can find a solution to the stochastic partial differential equation. The consistency and stability of the scheme are provided in the mean square sense. The scheme is conditionally stable, which means there are restrictions on time and space step sizes and parameters involved in given differential equations. The scheme will give a stable solution if step sizes are properly chosen. Otherwise, there will be no solution for each time level. An extra iterative scheme is considered since the Neumann-type boundary conditions are employed on each end of the boundary. So, the convergence of the scheme depends on the iterative scheme as well.

Figure 1 shows the flow chart of the presented methodology. Figure 2 compares three schemes for finding solutions to the deterministic diffusive model. The comparison is made with the non-standard finite difference method (NSFD) and the existing forward Euler method. The solution derived from the non-standard finite difference method exhibits minor discrepancies compared to the results obtained from the suggested and established Euler schemes. As demonstrated in Pasha et al. [50], the non-standard finite difference approach is only conditionally consistent, resulting in an issue with its order of accuracy. The non-standard finite difference method does not even provide an accurate first-order solution. Figure 3 compares the solutions of the deterministic and stochastic models obtained by the constructed scheme. Figure 4 shows the effect of the diffusion coefficient of the carbon dioxide equation. It can be concluded that the concentration of carbon dioxide rises as the diffusion coefficient escalates. Since carbon dioxide spreads over spatial variables, its concentration declines over time. Therefore, Figure 5 shows that carbon dioxide grows. The effect of the emission rate coefficient of CO_2 from the non-energy sector on the concentration of carbon dioxide is displayed in Figure 5. The concentration of CO_2 rises in the atmosphere as the emission rate coefficient of CO_2 from the non-energy sector grows. The higher coefficient means the increasing rate of carbon dioxide in the atmosphere. The next Figure 6 shows the effect of the emission rate coefficient of CO_2 from the energy sector on the concentration of CO_2 in atmosphere. The concentration goes up as the emission coefficient grows. Again, for the same reason, the coefficient increases mean a higher atmospheric concentration rate because of more carbon dioxide from the energy sector. The effect of population growth rate on population is shown in Figure 7. The population grows as the coefficient increases. Since the growth rate means more babies are born, the population increases; therefore, population growth graphs. The impact of the mortality rate coefficient on the population is depicted in Figure 8. Rising this coefficient means more people die, reducing the population, so the graph falls. The influence of the depletion rate of energy use on energy production is shown in Figure 9. The energy decreases as the depletion rate of energy use grows. A higher depletion rate means a decline in energy use, which brings down the graph. Figures 10 to 12 show the surfaces of concentration of carbon dioxide, human population, and energy production. These Figures 10 to 12 show how the variations in space and time affect the surfaces.

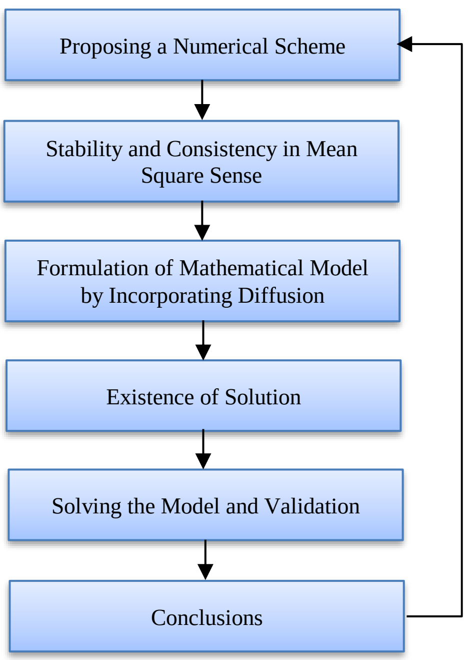

Figure 1. Flowchart of the methodology

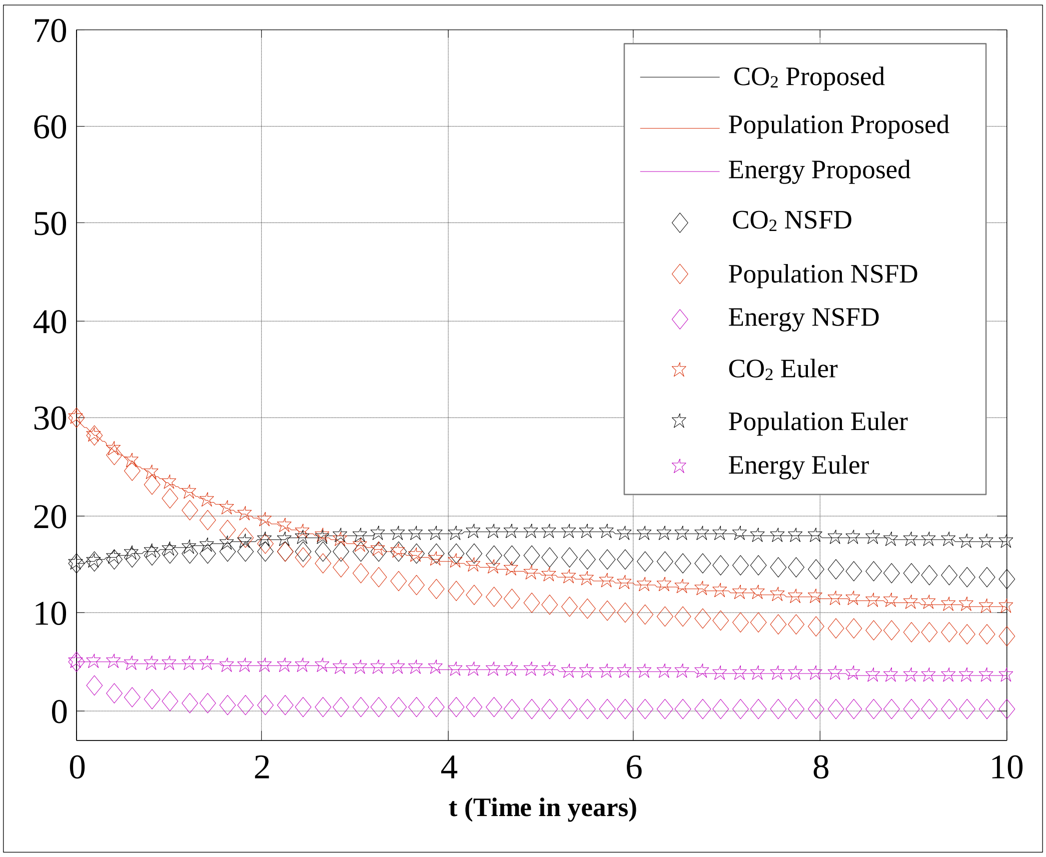

Figure 2. Comparison of three schemes for deterministic model using $d_1 = 0.3, d_2 = 0.1, d_3 = 0.3, C_o = 0.1, \alpha = 0.1, \lambda_1 = 0.1, \lambda_2 = 0.1, \mu = 0, r = 0.1, L = 5, \beta_1 = 0.01, \beta_2 = 0.001, \theta = 0, \nu = 0.1, \gamma = 0.01, K = 10, \gamma_o = 0.01$

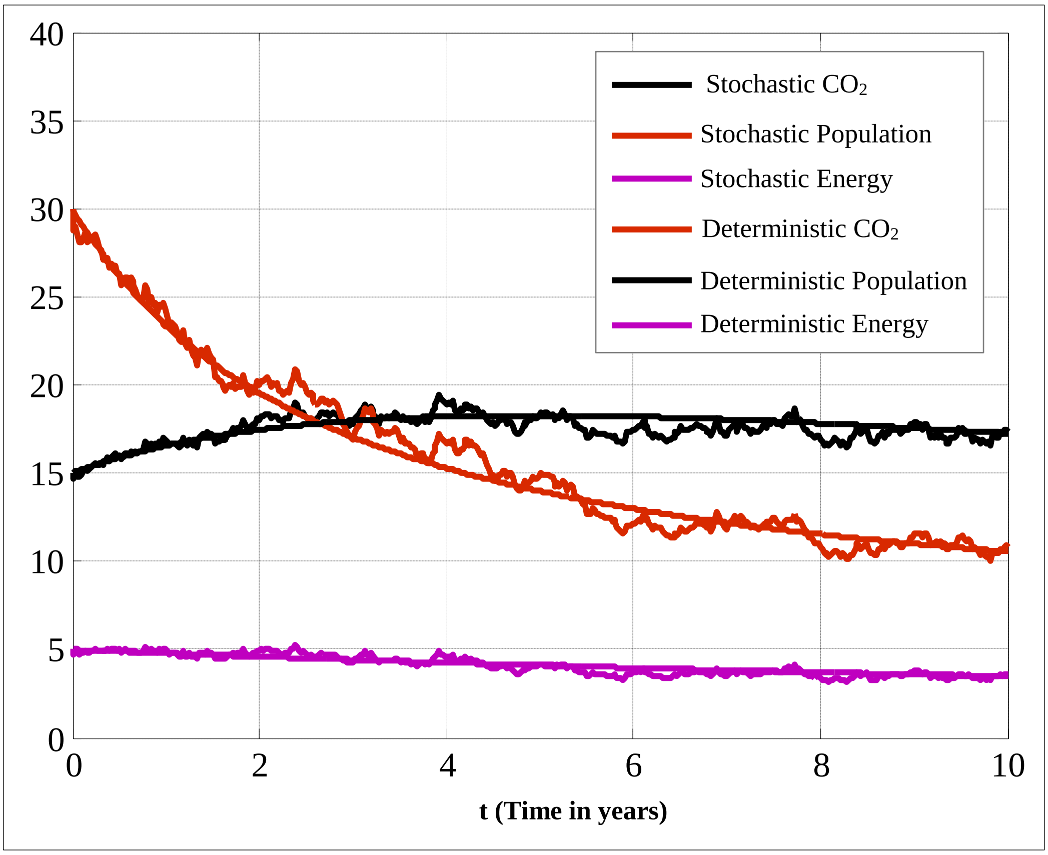

Figure 3. Comparison of stochastic and deterministic solutions using $d_1 = 0.3$, $d_2 = 0.1$, $d_3 = 0.3$, $C_o = 0.1, \alpha = 0.1, \lambda_1 = 0.1, \lambda_2 = 0.1$, $\mu = 0, r = 0.1$, $L = 5$, $\beta_1 = 0.01$, $\beta_2 = 0.001$, $\theta = 0$, $\nu = 0.1$, $\gamma = 0.01$, $K = 10$, $\gamma_o = 0.01, \sigma_1 = 0.07, \sigma_2 = 0.1, \sigma_3 = 0.15.$

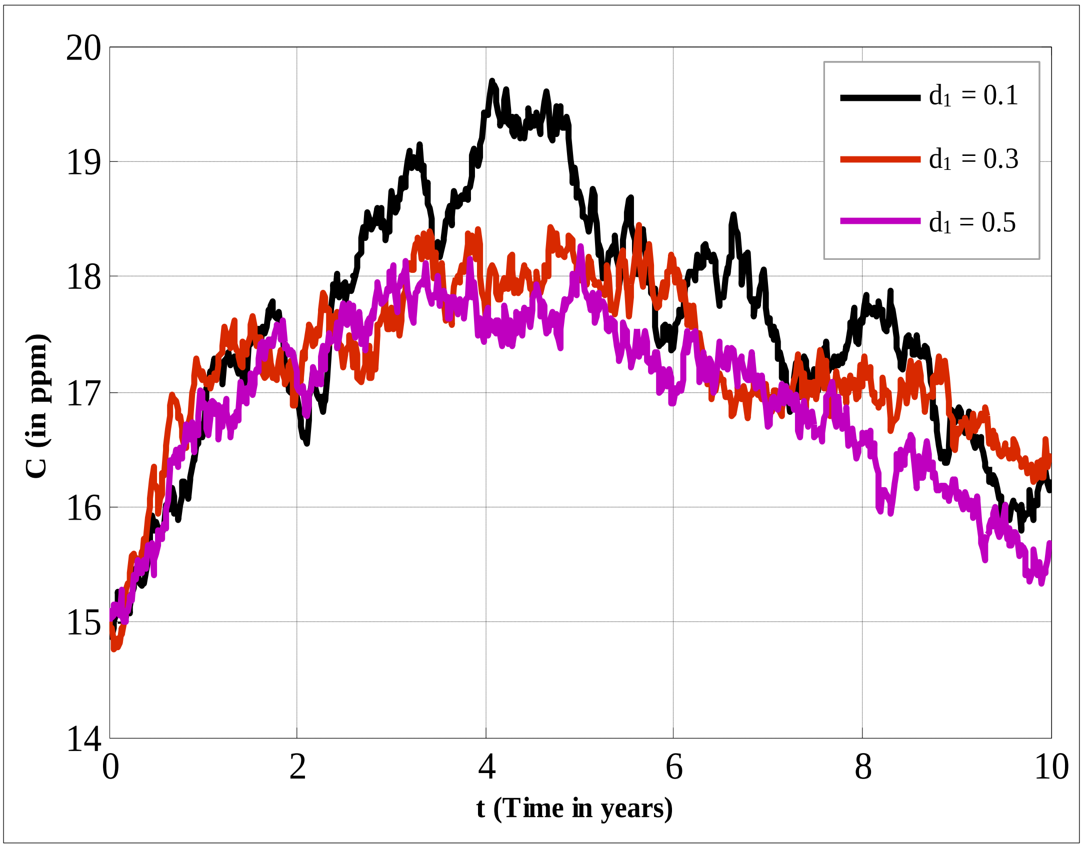

Figure 4. Effect of first diffusion coefficient on concentration of carbon dioxide using $d_2 = 0.1, d_3 = 0.3, C_o = 0.1, \alpha = 0.1, \lambda_1 = 0.1, \lambda_2 = 0.1, \mu = 0.01, r = 0.1, L = 5, \beta_1 = 0.01, \beta_2 = 0.001, \theta = 0.01, \nu = 0.1, \gamma = 0.01, K = 10, \gamma_o = 0.01, \sigma_1 = 0.05, \sigma_2 = 0.05, \sigma_3 = 0.05$

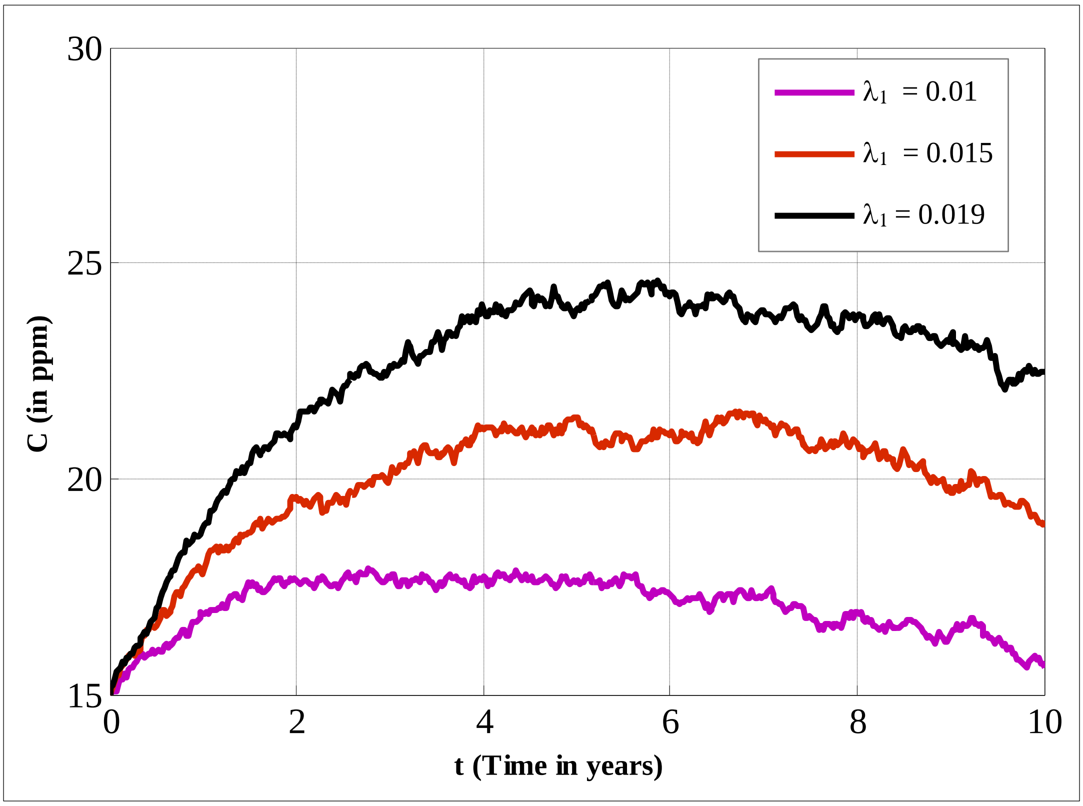

Figure 5. Effect of emission rate coefficient of CO_2 from non-energy sector on concentration of carbon dioxide using $d_2 = 0.1, d_3 = 0.3, C_o = 0.1, \alpha = 0.1, d_1 = 0.3, \lambda_2 = 0.1, \mu = 0.01, r = 0.1, L = 5, \beta_1 = 0.01, \beta_2 = 0.001, \theta = 0.01, \nu = 0.1, \gamma = 0.01, K = 10, \gamma_o = 0.01, \sigma_1 = 0.03, \sigma_2 = 0.03, \sigma_3 = 0.03$.

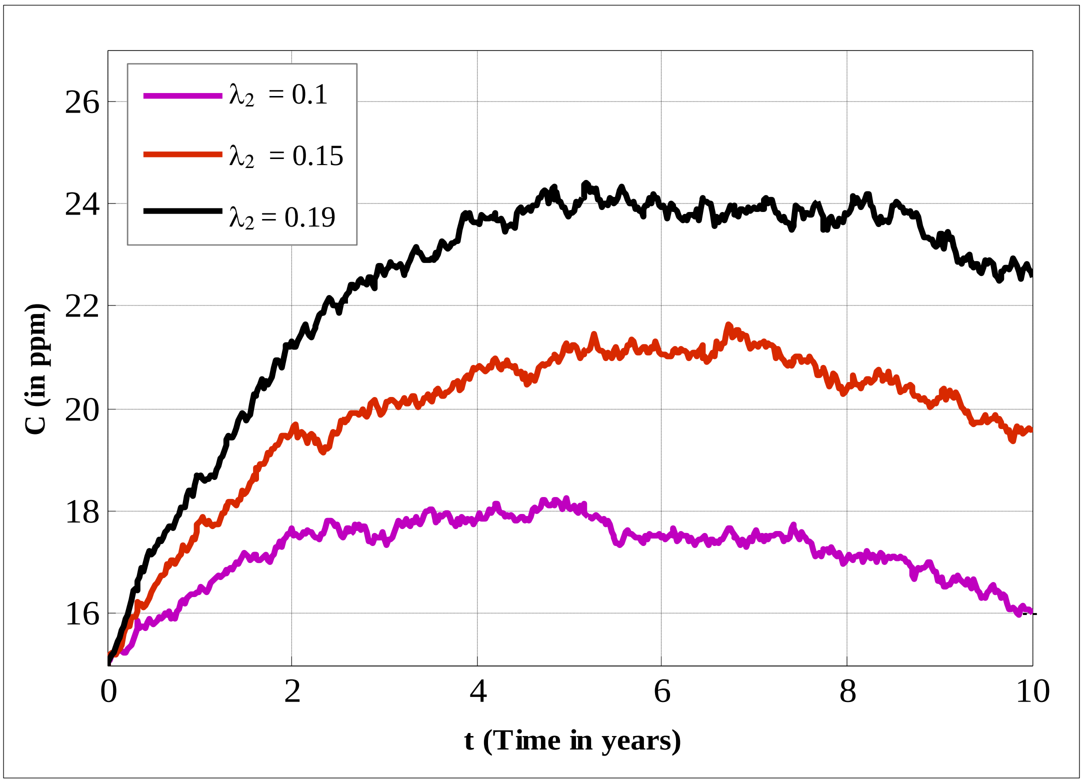

Figure 6. Effect of emission rate coefficient of CO_2 from energy sector on concentration of carbon dioxide using $d_2 = 0.1, d_3 = 0.3, C_o = 0.1, \alpha = 0.1, d_1 = 0.3, \lambda_1 = 0.1, \mu = 0.01, r = 0.1, L = 5, \beta_1 = 0.01, \beta_2 = 0.001, \theta = 0.01, \nu = 0.1, \gamma = 0.01, K = 10, \gamma_o = 0.01, \sigma_1 = 0.03, \sigma_2 = 0.03, \sigma_3 = 0.03$.

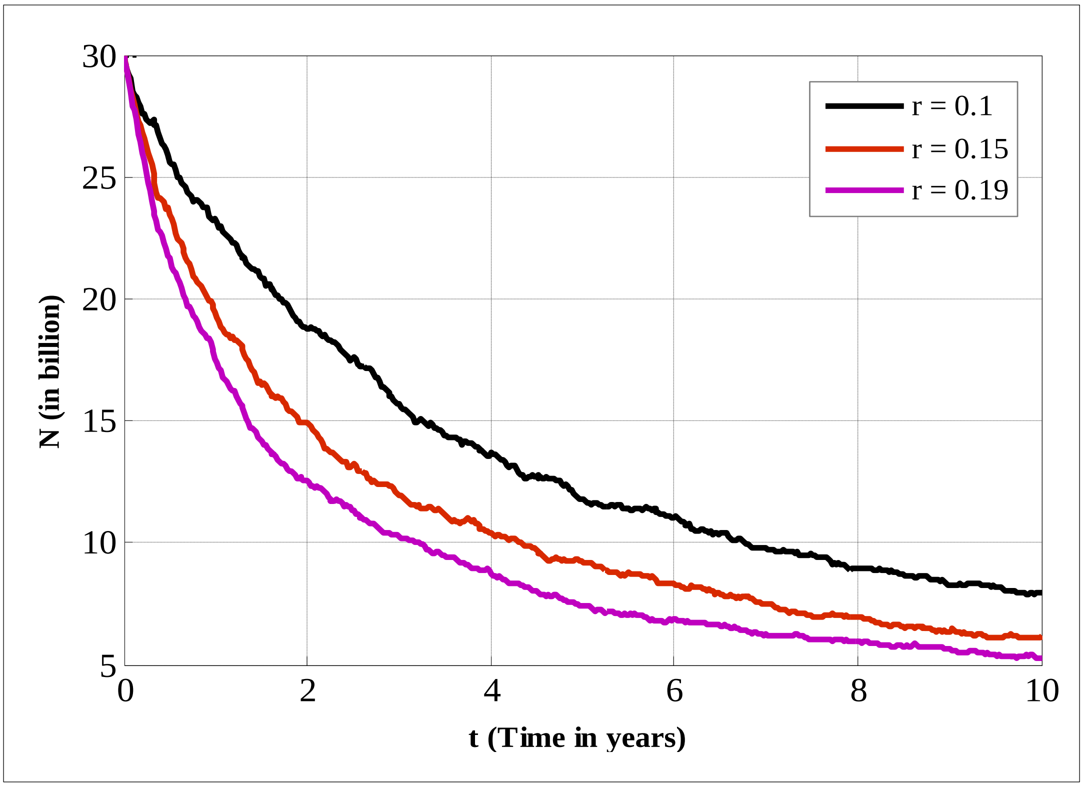

Figure 7. Effect of growth rate of population on population using $d_2 = 0.1, d_3 = 0.3, C_o = 0.1, \alpha = 0.1, d_1 = 0.3, \lambda_1 = 0.1, \mu = 0.01, \lambda_2 = 0.1, L = 5, \beta_1 = 0.01, \beta_2 = 0.001, \theta = 0.01, \nu = 0.1, \gamma = 0.01, K = 10, \gamma_o = 0.01, \sigma_1 = 0.03, \sigma_2 = 0.03, \sigma_3 = 0.03$.

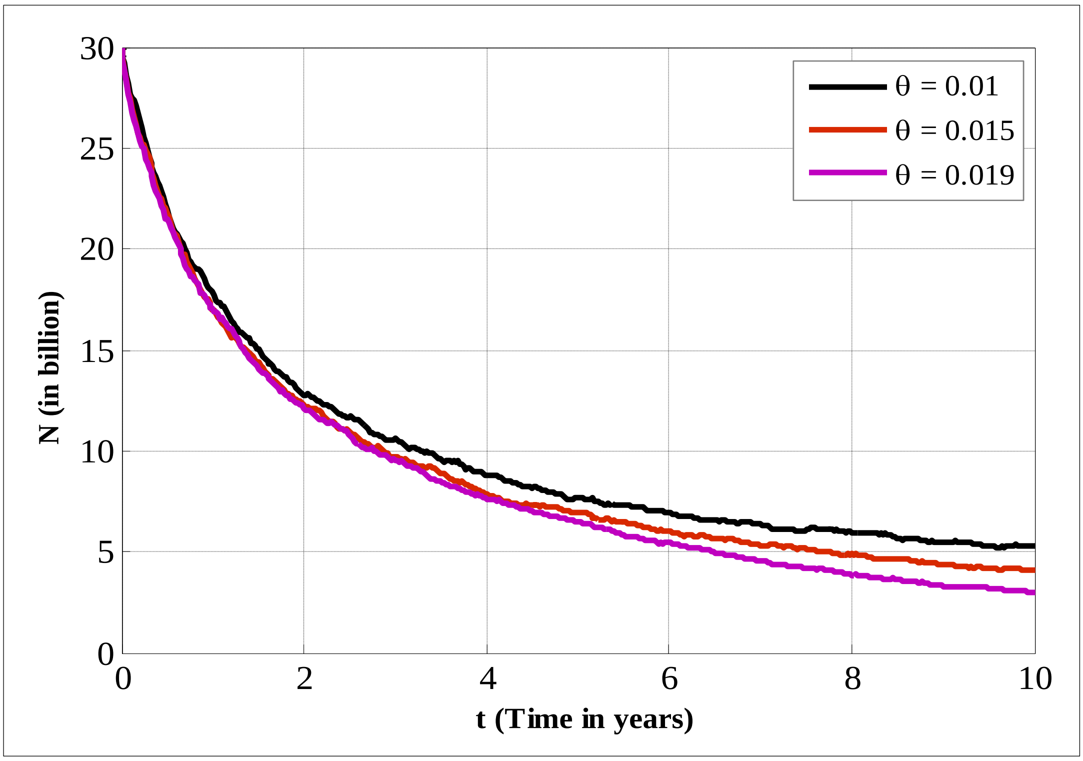

Figure 8. Effect of mortality rate of population on population using $d_2 = 0.1, d_3 = 0.3, C_o = 0.1, \alpha = 0.1, d_1 = 0.3, \lambda_1 = 0.1, \mu = 0.01, \lambda_2 = 0.1, L = 5, \beta_1 = 0.01, \beta_2 = 0.001, r = 0.019, \nu = 0.1, \gamma = 0.01, K = 10, \gamma_o = 0.01, \sigma_1 = 0.03, \sigma_2 = 0.03, \sigma_3 = 0.03$.

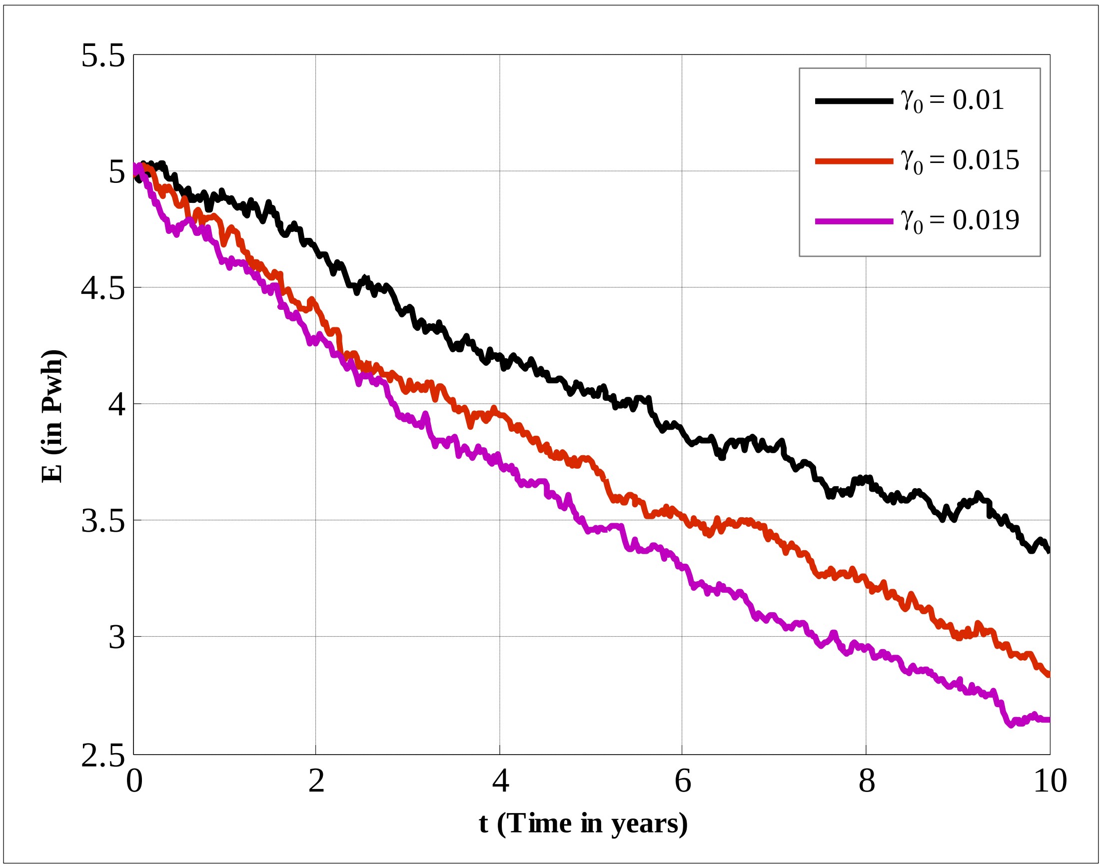

Figure 9. Effect of depletion rate of energy use on production of energy using $d_2 = 0.1, d_3 = 0.3, C_o = 0.1, \alpha = 0.1, d_1 = 0.3, \lambda_1 = 0.1, \mu = 0.01, \lambda_2 = 0.1, L = 5, \beta_1 = 0.01, \beta_2 = 0.001, r = 0.019, \nu = 0.1, \gamma = 0.01, K = 10, \theta = 0.01, \sigma_1 = 0.03, \sigma_2 = 0.03, \sigma_3 = 0.03$.

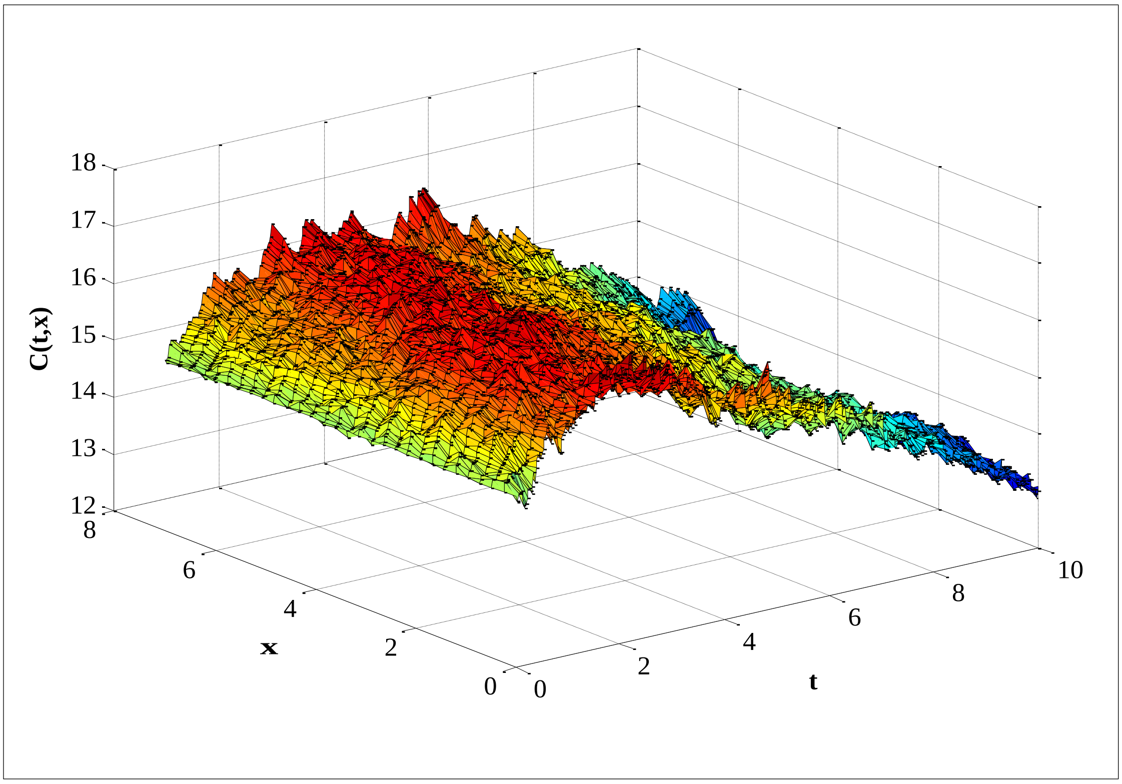

Figure 10. Surface plot for concentration of carbon dioxide using $d_2 = 0.1, d_3 = 0.3, C_o = 0.1, \alpha = 0.1, d_1 = 0.3, \lambda_1 = 0.1, \mu = 0.01, \lambda_2 = 0.1, L = 5, \beta_1 = 0.01, \beta_2 = 0.001, r = 0.019, \nu = 0.1, \gamma = 0.01, K = 10, \theta = 0.01, \gamma_o = 0.01, \sigma_1 = 0.03, \sigma_2 = 0.03, \sigma_3 = 0.03.$

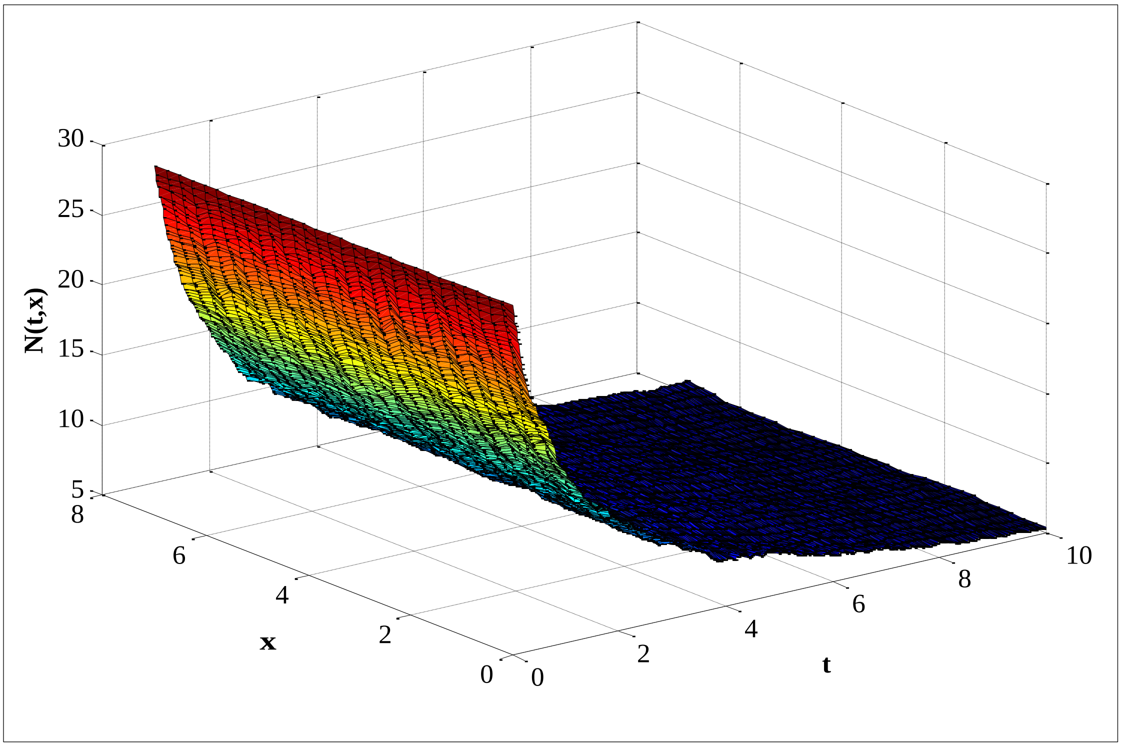

Figure 11. Surface plot for population using $d_2 = 0.1, d_3 = 0.3, C_o = 0.1, \alpha = 0.1, d_1 = 0.3, \lambda_1 = 0.1, \mu = 0.01, \lambda_2 = 0.1, L = 5, \beta_1 = 0.01, \beta_2 = 0.001, r = 0.019, \nu = 0.1, \gamma = 0.01, K = 10, \theta = 0.01, \gamma_o = 0.01, \sigma_1 = 0.03, \sigma_2 = 0.03, \sigma_3 = 0.03.$

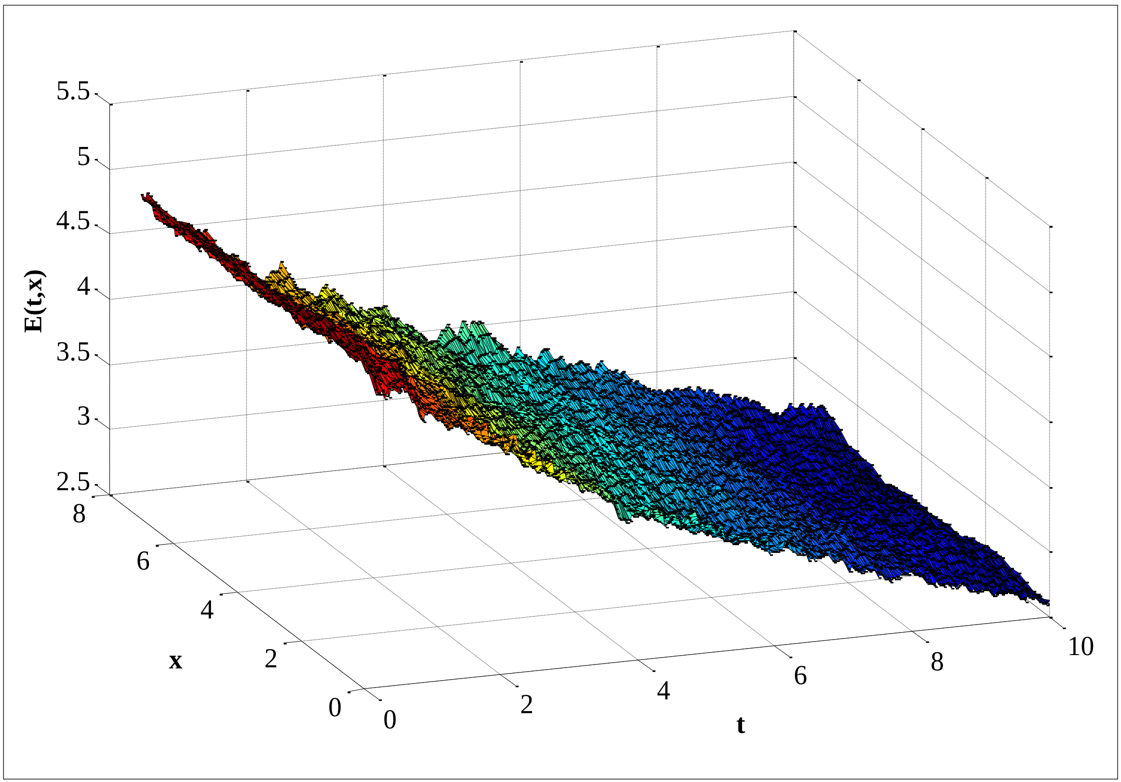

Figure 12. **Surface plot for production of energy using** $d_2 = 0.1, d_3 = 0.3, C_o = 0.1, \alpha = 0.1, d_1 = 0.3, \lambda_1 = 0.1, \mu = 0.01, \lambda_2 = 0.1, L = 5, \beta_1 = 0.01, \beta_2 = 0.001, r = 0.019, \nu = 0.1, \gamma = 0.01, K = 10, \theta = 0.01, \gamma_o = 0.01,\ \sigma_1 = 0.03, \sigma_2 = 0.03, \sigma_3 = 0.03$.

Table 1 shows the comparison of two schemes for finding L_2 error of Equation 1 using $G = 0$. Two different numerical schemes are used for finding this error. The second order central difference formula does the space discretization for proposed scheme. This Table 1 shows that the proposed scheme performs better than the existing non-standard finite difference method.

Table 1. **Comparison of existing and proposed scheme for finding norm of error using** $d_1 = 0.1,\ c = 500,\ N_x(grid\ points) = 50,\ t_f = 1$

Δt	L_2 Error	
	Proposed	**NSFD**
1/200	0.1412	0.2433
1/300	0.1901	0.2350
1/400	0.2321	0.2571
1/500	0.2688	0.2852

5- Conclusions

This project aims to improve the computational resources for studying and modeling the stochastic diffusive dynamics of energy production, human population, and carbon dioxide concentration. The suggested numerical methodology, which expands the Euler-Maruyama method, helps solve stochastic time-dependent PDEs. In environmental systems with inherent uncertainties and random variations, the consistency and stability shown in the mean square sense enhance the scheme's trustworthiness and applicability. A giant leap forward in our ability to comprehend environmental processes has been made possible by updating an earlier mathematical model to include stochastic components and diffusion effects. Our model provides a more accurate depiction of the complicated dynamics influencing trends in CO_2 concentration, population dynamics, and energy production patterns by considering these elements. These components interact in a complex and interconnected manner. A stochastic computational scheme has been constructed to handle time-dependent partial differential equations with the effects of random variations. The random terms in differential equations were based on Wiener processes. The Matlab command handles these Wiener process terms as a random number of Normal distributions. Our suggested stochastic scheme is numerically more accurate, as shown by a comparison with an existing non-standard finite difference method. Considering the accuracy order, the scheme's improved performance becomes more apparent, highlighting its promise as a trustworthy tool for replicating real-world situations. The contribution of both energy and non-energy sectors to environmental outcomes can be better understood through research on the effect of emission rate coefficients on CO_2 concentration. The concluding points can be expressed as:

- Compared to the current non-standard finite difference method, the suggested scheme achieved a higher level of accuracy.
- The concentration of carbon dioxide was raised as emission rate coefficients of non-energy and energy sectors were grown.
- The production of energy declines as the depletion rate of energy use is raised.

Our research contributes to what is known to create more realistic and complicated environmental models in the face of climate change's various challenges. Researchers and policymakers can gain deeper insights into human activities' ecological impacts using the recommended computer method and enhanced mathematical model [51-53]. We develop robust models for stochastic and diffusive processes to enable sustainable environmental management and informed decision-making.

6- Declarations

6-1- Author Contributions

Conceptualization, Y.N. and M.S.A.; methodology, Y.N.; software, Y.N.; validation, M.S.A., K.A., and H.M.A.; formal analysis, M.S.A.; investigation, H.M.A.; resources, K.A.; data curation, H.M.A.; writing—original draft preparation, M.S.A.; writing—review and editing, Y.N.; visualization, H.M.A.; supervision, M.S.A.; project administration, K.A.; funding acquisition, H.M.A. All authors have read and agreed to the published version of the manuscript.

6-2- Data Availability Statement

The data presented in this study are available in the article.

6-3- Funding

The authors would like to acknowledge the support of Prince Sultan University for paying the article processing charges of this publication.

6-4- Acknowledgements

The authors wish to express their gratitude to Prince Sultan University for facilitating the publication of this article through the Theoretical and Applied Sciences Lab.

6-5- Institutional Review Board Statement

Not applicable.

6-6- Informed Consent Statement

Not applicable.

6-7- Conflicts of Interest

The authors declare that there is no conflict of interest regarding the publication of this manuscript. In addition, the ethical issues, including plagiarism, informed consent, misconduct, data fabrication and/or falsification, double publication and/or submission, and redundancies have been completely observed by the authors.

7- References

[1] Tian, Y., Sun, K., Chen, L., & Kasperski, A. (2010). Studies on the dynamics of a continuous bioprocess with impulsive state feedback control. Chemical Engineering Journal, 157(2–3), 558–567. doi:10.1016/j.cej.2010.01.002.

[2] Yang, J., & Tang, G. (2019). Piecewise chemostat model with control strategy. Mathematics and Computers in Simulation, 156, 126–142. doi:10.1016/j.matcom.2018.07.004.

[3] Pilling, M. J. (1989). Mathematical Models of Chemical Reactions. Theory and Applications of Deterministic and Stochastic Models. Journal of Photochemistry and Photobiology A: Chemistry, 49(3), 409–410. doi:10.1016/1010-6030(89)87138-2.

[4] Zhao, Z., Zhang, X., & Chen, L. (2010). Nonlinear modelling of chemostat model with time delay and impulsive effect. Nonlinear Dynamics, 63(1–2), 95–104. doi:10.1007/s11071-010-9788-1.

[5] Kilbas, A. A., Srivastava, H. M., & Trujillo, J. J. (2006). Theory and applications of fractional differential equations. Elsevier, Amsterdam, Netherlands.

[6] Podlubny, I. (1999). Fractional differential equations, mathematics in science and engineering. Academic Press, Washington, United States.

[7] Khan, N. A., Hameed, T., Khan, N. A., & Raja, M. A. Z. (2018). A heuristic optimization method of fractional convection reaction an application to diffusion process. Thermal Science, 22, S243–S252. doi:10.2298/TSCI170717292K.

[8] Puliyanda, A., Srinivasan, K., Li, Z., & Prasad, V. (2023). Benchmarking chemical neural ordinary differential equations to obtain reaction network-constrained kinetic models from spectroscopic data. Engineering Applications of Artificial Intelligence, 125, 125 106690. doi:10.1016/j.engappai.2023.106690.

[9] Rossikhin, Y. A., & Shitikova, M. V. (1997). Applications of fractional calculus to dynamic problems of linear and nonlinear hereditary mechanics of solids. Applied Mechanics Reviews, 50(1), 15–67. doi:10.1115/1.3101682.

[10] Bao, L., Dai, C., Liu, C., Jia, Y., Liu, X., Ren, X., Ali, S., Bououdina, M., & Zeng, C. (2024). Fluorine lattice-doped ZnS with accompanying sulfur vacancies for high activity and selectivity of CO_2 conversion to CO. Ceramics International, 50(11), 19769–19780. doi:10.1016/j.ceramint.2024.03.100.

[11] Ali, S., Ismail, P. M., Humayun, M., Bououdina, M., & Qiao, L. (2024). Tailoring 2D metal-organic frameworks for enhanced CO_2 reduction efficiency through modulating conjugated ligands. Fuel Processing Technology, 255, 108049. doi:10.1016/j.fuproc.2024.108049.

[12] Liu, J., Liu, X., Dai, C., Zeng, C., Ali, S., Bououdina, M., & Jia, Y. (2024). Copper-doped Bi2MoO6 with concurrent oxygen vacancies for enhanced CO_2 photoreduction. Inorganic Chemistry Frontiers, 11(22), 8003–8015. doi:10.1039/d4qi02005g.

[13] BP International (2019). BP Statistical Review of World Energy 2019: an unsustainable path. BP International, London, United Kingdom. Available online: https://www.bp.com/en/global/corporate/news-and-insights/press-releases/bp-statistical-review-of-world-energy-2019.html (accessed on January 2025)

[14] DOW/EIA-0484. (2013). International Energy Outlook 2013. U.S. Energy Information Administration, Office of Energy Analysis, U.S. Department of Energy, Washington, United States.

[15] EPA. (2019). Inventory of U.S. Greenhouse Gas Emissions and Sinks: 1990-2017. U.S. Environmental Protection Agency, Washington, United States.

[16] Zabel, G. (2009). Peak People: The Interrelationship between Population Growth and Energy Resources - Resilience. Energy Bulletin. Available online: https://www.resilience.org/stories/2009-04-20/peak-people-interrelationship-between-population-growth-and-energy-resources/ (accessed on January 2025).

[17] Nikol'skii, M. S. (2010). A controlled model of carbon circulation between the atmosphere and the ocean. Computational Mathematics and Modeling, 21(4), 414–424. doi:10.1007/s10598-010-9081-7.

[18] Emami, M. J., Tang, Y., Wang, Z., & Tontiwachwuthikul, P. (2023). Forecast energy demand, CO_2 emissions and energy resource impacts for the transportation sector: – Multi-objective optimization, sensitivity analysis and Canada Case Study. Applied Energy, 338, 120830. doi:10.1016/j.apenergy.2023.120830.

[19] Weng, Z., Song, Y., Ma, H., Ma, Z., & Liu, T. (2023). Forecasting energy demand, structure, and CO_2 emission: a case study of Beijing, China. Environment, Development and Sustainability, 25(9), 10369–10391. doi:10.1007/s10668-022-02494-1.

[20] Caetano, M. A. L., Gherardi, D. F. M., & Yoneyama, T. (2011). An optimized policy for the reduction of CO_2 emission in the Brazilian Legal Amazon. Ecological Modelling, 222(15), 2835–2840. doi:10.1016/j.ecolmodel.2011.05.003.

[21] Misra, A. K., & Verma, M. (2013). A mathematical model to study the dynamics of carbon dioxide gas in the atmosphere. Applied Mathematics and Computation, 219(16), 8595–8609. doi:10.1016/j.amc.2013.02.058.

[22] Misra, A. K., Verma, M., & Venturino, E. (2015). Modeling the control of atmospheric carbon dioxide through reforestation: effect of time delay. Modeling Earth Systems and Environment, 1(3), 24. doi:10.1007/s40808-015-0028-z.

[23] Beér, J. M. (2007). High efficiency electric power generation: The environmental role. Progress in Energy and Combustion Science, 33(2), 107–134. doi:10.1016/j.pecs.2006.08.002.

[24] Liu, T., Xu, G., Cai, P., Tian, L., & Huang, Q. (2011). Development forecast of renewable energy power generation in China and its influence on the GHG control strategy of the country. Renewable Energy, 36(4), 1284–1292. doi:10.1016/j.renene.2010.09.020.

[25] Jin, S. H., Bai, L., Kim, J. Y., Jeong, S. J., & Kim, K. S. (2017). Analysis of GHG emission reduction in South Korea using a CO_2 transportation network optimization model. Energies, 10(7), 1027. doi:10.3390/en10071027.

[26] Yoro, K. O., & Sekoai, P. T. (2016). The potential of CO_2 capture and storage technology in South Africa's coal-fired thermal power plants. Environments, 3(3), 1–20. doi:10.3390/environments3030024.

[27] Mesarić, P., Dukec, D., & Krajcar, S. (2017). Exploring the potential of energy consumers in smart grid using focus group methodology. Sustainability (Switzerland), 9(8), 9. doi:10.3390/su9081463.

[28] Siano, P. (2014). Demand response and smart grids - A survey. Renewable and Sustainable Energy Reviews, 30, 461–478. doi:10.1016/j.rser.2013.10.022.

[29] Shi, J., Wang, Y., Fu, R., & Zhang, J. (2017). Operating strategy for local-area energy systems integration considering uncertainty of supply-side and demand-side under conditional value-at-risk assessment. Sustainability (Switzerland), 9(9), 9. doi:10.3390/su9091655.

[30] Adnani, J., Hattaf, K., & Yousfi, N. (2013). Stability Analysis of a Stochastic SIR Epidemic Model with Specific Nonlinear Incidence Rate. International Journal of Stochastic Analysis, 431257, 1–4. doi:10.1155/2013/431257.

[31] Alzabut, J., Alobaidi, G., Hussain, S., Madi, E. N., & Khan, H. (2022). Stochastic dynamics of influenza infection: Qualitative analysis and numerical results. Mathematical Biosciences and Engineering, 19(10), 10316–10331. doi:10.3934/mbe.2022482.

[32] Hussain, S., Madi, E. N., Khan, H., Gulzar, H., Etemad, S., Rezapour, S., & Kaabar, M. K. A. (2022). On the Stochastic Modeling of COVID-19 under the Environmental White Noise. Journal of Function Spaces, 2022, 4320865. doi:10.1155/2022/4320865.

[33] Gao, M., Jiang, D., & Hayat, T. (2019). Stationary distribution and periodic solution of stochastic chemostat models with single-species growth on two nutrients. International Journal of Biomathematics, 12(6), 1950063. doi:10.1142/S1793524519500633.

[34] Liu, Q., Jiang, D., Hayat, T., & Ahmad, B. (2017). Asymptotic behavior of a stochastic delayed HIV-1 infection model with nonlinear incidence. Physica A: Statistical Mechanics and Its Applications, 486, 867–882. doi:10.1016/j.physa.2017.05.069.

[35] Zhang, T., & Teng, Z. (2008). An impulsive delayed SEIRS epidemic model with saturation incidence. Journal of Biological Dynamics, 2(1), 64–84. doi:10.1080/17513750801894845.

[36] Xu, R., & Ma, Z. (2009). Global stability of a SIR epidemic model with nonlinear incidence rate and time delay. Nonlinear Analysis: Real World Applications, 10(5), 3175–3189. doi:10.1016/j.nonrwa.2008.10.013.

[37] Mikhaylov, A. N., Guseinov, D. V., Belov, A. I., Korolev, D. S., Shishmakova, V. A., Koryazhkina, M. N., Filatov, D. O., Gorshkov, O. N., Maldonado, D., Alonso, F. J., Roldán, J. B., Krichigin, A. V., Agudov, N. V., Dubkov, A. A., Carollo, A., & Spagnolo, B. (2021). Stochastic resonance in a metal-oxide memristive device. Chaos, Solitons & Fractals, 144, 110723. doi:10.1016/j.chaos.2021.110723.

[38] Gawusu, S., & Ahmed, A. (2024). Analyzing variability in urban energy poverty: A stochastic modeling and Monte Carlo simulation approach. Energy, 304, 132194. doi:10.1016/j.energy.2024.132194.

[39] Lisowski, B., Valenti, D., Spagnolo, B., Bier, M., & Gudowska-Nowak, E. (2015). Stepping molecular motor amid Lévy white noise. Physical Review E - Statistical, Nonlinear, and Soft Matter Physics, 91, 042713. doi:10.1103/PhysRevE.91.042713.

[40] Jamatutu, S. A., Abbass, K., Gawusu, S., Yeboah, K. E., Jamatutu, I. A. M., & Song, H. (2024). Quantifying future carbon emissions uncertainties under stochastic modeling and Monte Carlo simulation: Insights for environmental policy consideration for the Belt and Road Initiative Region. Journal of Environmental Management, 370, 122463. doi:10.1016/j.jenvman.2024.122463.

[41] Surazhevsky, I. A., Demin, V. A., Ilyasov, A. I., Emelyanov, A. V., Nikiruy, K. E., Rylkov, V. V., Shchanikov, S. A., Bordanov, I. A., Gerasimova, S. A., Guseinov, D. V., Malekhonova, N. V., Pavlov, D. A., Belov, A. I., Mikhaylov, A. N., Kazantsev, V. B., Valenti, D., Spagnolo, B., & Kovalchuk, M. V. (2021). Noise-assisted persistence and recovery of memory state in a memristive spiking neuromorphic network. Chaos, Solitons and Fractals, 146, 110890. doi:10.1016/j.chaos.2021.110890.

[42] Abudureheman, M., Jiang, Q., Dong, X., & Dong, C. (2022). Spatial effects of dynamic comprehensive energy efficiency on CO_2 reduction in China. Energy Policy, 166, 113024. doi:10.1016/j.enpol.2022.113024.

[43] Xie, Q., Ma, D., Raza, M. Y., Tang, S., & Bai, D. (2023). Toward carbon peaking and neutralization: The heterogeneous stochastic convergence of CO_2 emissions and the role of digital inclusive finance. Energy Economics, 125, 106841. doi:10.1016/j.eneco.2023.106841.

[44] Yang, C., Bu, S., Fan, Y., Wan, W. X., Wang, R., & Foley, A. (2023). Data-driven prediction and evaluation on future impact of energy transition policies in smart regions. Applied Energy, 332, 120523. doi:10.1016/j.apenergy.2022.120523.

[45] Valenti, D., Denaro, G., La Cognata, A., Spagnolo, B., Bonanno, A., Basilone, G., Mazzola, S., Zgozi, S., & Aronica, S. (2012). Picophytoplankton dynamics in noisy marine environment. Acta Physica Polonica B, 43(5), 1227–1240. doi:10.5506/APhysPolB.43.1227.

[46] Chichigina, O. A., Dubkov, A. A., Valenti, D., & Spagnolo, B. (2011). Stability in a system subject to noise with regulated periodicity. Physical Review E: Statistical, Nonlinear, and Soft Matter Physics, 84(2), 21134. doi:10.1103/PhysRevE.84.021134.

[47] Bonanno, G., Valenti, D., & Spagnolo, B. (2006). Role of noise in a market model with stochastic volatility. European Physical Journal B, 53(3), 405–409. doi:10.1140/epjb/e2006-00388-1.

[48] Valenti, D., Fazio, G., & Spagnolo, B. (2018). Stabilizing effect of volatility in financial markets. Physical Review E, 97(6), 062307. doi:10.1103/PhysRevE.97.062307.

[49] Verma, M., Verma, A. K., & Misra, A. K. (2021). Mathematical modeling and optimal control of carbon dioxide emissions from energy sector. Environment, Development and Sustainability, 23(9), 13919–13944. doi:10.1007/s10668-021-01245-y.

[50] Pasha, S. A., Nawaz, Y., & Arif, M. S. (2023). On the nonstandard finite difference method for reaction–diffusion models. Chaos, Solitons & Fractals, 166, 112929. doi:10.1016/j.chaos.2022.112929.

[51] Baazeem, A. S., Nawaz, Y., Arif, M. S., Abodayeh, K., & AlHamrani, M. A. (2023). Modelling Infectious Disease Dynamics: A Robust Computational Approach for Stochastic SIRS with Partial Immunity and an Incidence Rate. Mathematics, 11(23), 4794. doi:10.3390/math11234794.

[52] Arif, M. S., Abodayeh, K., & Nawaz, Y. (2024). A Third-order Two Stage Numerical Scheme and Neural Network Simulations for SEIR Epidemic Model: A Numerical Study. Emerging Science Journal, 8(1), 326–340. doi:10.28991/ESJ-2024-08-01-023.

[53] Arif, M. S., Abodayeh, K., & Nawaz, Y. (2024). Precision in disease dynamics: Finite difference solutions for stochastic epidemics with treatment cure and partial immunity. Partial Differential Equations in Applied Mathematics, 9, 100660. doi:10.1016/j.padiff.2024.100660.